Proc. Symposium IEEE Benelux Chapter on Communications
and Vehicular Technology, 2004 (SCVT2004),
Gent, Belgium, Nov. 2004.

Throughput of a MIMO OFDM based WLAN system

Tim C.W. Schenk*‡, Guido Dolmans† and Isabella Modonesi*
*Agere Systems, PO Box 755, 3430 AT Nieuwegein, The Netherlands.
‡Eindhoven University of Technology, PO Box 513, 5600 MB Eindhoven, The Netherlands, T.C.W.Schenk@tue.nl.
†Philips Research Laboratories, Prof. Holstlaan 4, 5656 AA Eindhoven, The Netherlands, Guido.Dolmans@philips.com.

***Abstract*— In this paper, the system throughput of a wireless local-area-network (WLAN) based on multiple-input multiple-output orthogonal frequency division multiplexing (MIMO OFDM) is studied. A broadband channel model is derived from indoor channel measurements. This model is used in simulations to evaluate the performance of different MIMO detection algorithms. It is concluded that a MIMO scheme combined with an additional antenna at the receiver side and the low computational complex minimum-mean-squared-error (MMSE) algorithm is preferable. Link-level results are used to calculate the throughput of a single-cell scenario containing multiple MIMO users using a semi-analytical framework. Results show that the throughput of a 2×2 extension of an IEEE 802.11a system is 1.5 to 2 times higher than that of its single antenna counterpart.**

I. Introduction

Over the last few years the application of multiple antennas at both transmitter (TX) and receiver (RX) side of a wireless system is proposed in many publications, e.g., [1], [2]. The combination of these multiple-input multiple-output (MIMO) techniques with orthogonal frequency division multiplexing (OFDM) for broadband systems is seen as a promising basis for next-generation high data rate wireless systems [3]. This is especially the case for wireless local-area-networks (WLAN), which more and more are based on the IEEE standards 802.11a [4] and 802.11g [5], since they already use OFDM. The potential of this physical layer design has led to a high number of proposals for the high data rate IEEE 802.11n, which are based on this concept. Furthermore, several papers appeared recently showing successful (test) implementations of MIMO applied for different wireless communication systems, e.g., [6]–[9], proving merits of the concept.

Unlike most of the literature in the field, only focused on propagation and signal processing aspects of MIMO systems, this paper investigates the potential of MIMO in providing increased throughput in a multi-terminal WLAN system environment. First channel measurements were carried out in an indoor environment, which were the basis for a broadband MIMO channel model. This model was used to simulate the bit-error-rate (BER) and packet-error-rate (PER) performance of several single-user MIMO configurations applying different MIMO detectors, modulations and coding rates. As a trade-off between computational complexity and performance, a preferred detection scheme is proposed in this paper.

To find the throughput of a multi-terminal environment, a theoretical framework has to be developed to incorporate these single-user PER results into a system-level model. The common way-of-working to implement system-level models is to use commercial numerical simulation tools like OPNET, see e.g. [10]. In these tools, however, the system is built according to the OSI stack with time-consuming implementations of PHY, medium access control (MAC), network and application layers. Here we are only interested in the variations in throughput due to small-scale fading, path loss and the WLAN cell size. To analyze these basic effects, a semi-analytical approach is adopted, based on [11]. We specifically address the uplink throughput versus the WLAN cell size without intra- and intercell interference; however, a downlink analysis and/or adding interference can be analyzed with the same approach. A different semi-analytical approach to derive throughput including interference, applied to smart-antenna beamforming, can be found in [12]. None of the semi-analytical system models in literature are to the best of the authors' knowledge applied to MIMO systems.

The organization of the paper is as follows. Section II describes how a broadband channel model is derived from channel measurements. The system model for a system combining MIMO with OFDM is explained in Section III. Applying the channel model, the performance of different MIMO detection algorithms is evaluated in Section IV. These results are used in Section V to analyze the system throughput. Finally, conclusions are drawn in Section VI.

II. Broadband MIMO channel measurements

Statistical characterization of the radio channel is needed for the design of a broadband MIMO wireless system. Therefore, broadband channel measurements were carried out in a lab-room ($14\times11\times2.7$ m^3) at Philips Research, Eindhoven, The Netherlands. The measurements were obtained with a 4×4 MIMO test-bed, designed for the 5.8 GHz ISM band, which is further described in [13]. The measurements were carried using an automated X-Y scanner, which enabled analysis of MIMO fading channels on a small-scale basis. The 4 TX antennas were connected via RF and IF chains to multiple D/A cards and the 5.8 GHz signals with a 20 MHz bandwidth were transmitted over the air. The 4 RX antennas were placed such that they were not facing the TX antennas; the antenna arrays illuminated the walls. Therefore, the transmitted signals experienced multipath fading before being captured at the receiver. The test-bed simultaneously radiated 4 symbol streams over the air and the complex channel matrix was captured at 1650 spatial points using the 4 RX antennas. For the data captured at each position, the channel elements were computed with 17 taps in time, the spacing between taps was 50 ns.

From the measurement results the spatial correlation was concluded to be low, with a mean of 0.13 and a maximum of 0.3. [14] shows that the influence of such correlation values on system performance is negligible. Therefore, correlation effects were not taken into account in the final channel model. The mean value of the rms delay spread was found to be 30 ns. The fading of both the main and other taps was found to agree well to Rayleigh fading. The power-delay-profile (PDP) was found to exhibit an exponential decay. The final channel model, based on these findings, is reported in [15]. It distinguishes 5 scenarios with different delay spreads. For the indoor environment, regarded in this paper, the rms delay spread values are 10 ns, 30 ns and 50 ns, modelling the 1 percentile, the mean and the 99 percentile case, respectively.

III. System model description

Since increase of the data rate of current WLAN systems is the main goal of this work, we regard the space division multiplexing (SDM) flavor from the group of MIMO schemes. In SDM independent data streams are transmitted from the N_t different TX antennas.

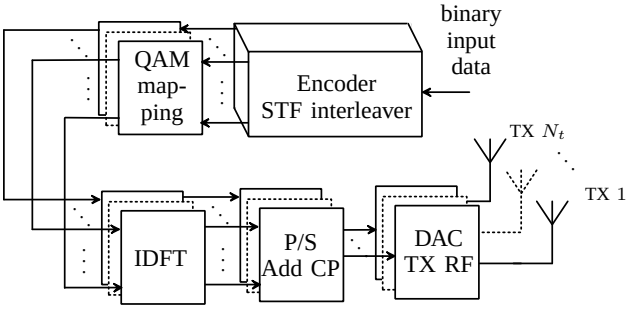

Fig. 1. MIMO OFDM transmitter model.

Figure 1 depicts the block scheme of a typical structure of a system combining SDM with OFDM. The binary input data is encoded and interleaved. Two ways of channel encoding are regarded: joint coding (JC), where the symbols are interleaved after encoding and per antenna coding (PAC), where the data stream is demultiplexed to the different TX branches before encoding. In the latter case the encoding is done per branch. After encoding and space-time-frequency (STF) interleaving the data is mapped to complex quadrature amplitude modulation (QAM) symbols. These symbols are transformed to the time domain using the inverse discrete fourier transform (IDFT). After parallel-to-serial (P/S) conversion a cyclic prefix (CP) is added to increase multipath robustness. After conversion from digital to analog, the signals are upconverted to radio frequency (RF) and transmitted through the N_t antennas.

Figure 2 depicts the system model of a typical SDM OFDM receiver. The signals received at the N_r receiver antennas are down-converted to baseband and sampled. From the digital data streams the CP is removed, to decrease the influence of the multipath induced inter-symbol-interference (ISI). After serial-to-parallel (S/P) conversion the signals are transformed to the frequency domain using the DFT. Then MIMO detection

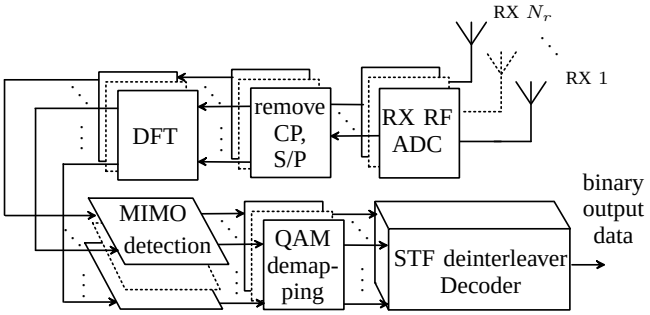

Fig. 2. MIMO OFDM receiver model.

is applied to every subcarrier, separately. This recovers the N_t transmitted symbols from the N_r received symbols, per subcarrier. The QAM demapper then converts the detected complex symbols to binary data streams. Finally, the data is deinterleaved and decoded. Again the order depends on the chosen encoding method, i.e., JC or PAC.

IV. Link level simulations

A. Simulation parameters

The evaluation of the performance of different MIMO detectors is focussed on four different detection methods. Two based on linear estimation theory, i.e., zero-forcing (ZF) and minimum-mean-squared-error (MMSE), one on a linear estimator combined with feedback, i.e., vertical BLAST (VBLAST), and the non-linear maximum likelihood detector (MLD). A comprehensive description and complexity analysis of these detection schemes is given in [14].

Since the purpose of the research was to compare the performance of different detection schemes and antenna configurations, a system only impaired by additive white Gaussian noise (AWGN) was regarded. In the simulations the TX and RX are, therefore, perfectly synchronized and perfect knowledge about the MIMO channel is available at the RX side of the system. The decoder applies soft decision values from the QAM demapper as input. The channel is assumed quasi-static, which means the channel responses do not change during the reception of one packet. The signal parameters are based on those of the 802.11a standard, as summarized in Table I.

TABLE I
Simulation parameters, based on IEEE 802.11a

System Parameter	Parameter Value
Bandwidth	20 MHz
Modulation	BPSK, QPSK, 16QAM, 64QAM
Coding	Convolutional
Number of subcarriers	64
Number of data subcarriers	48
Number of pilot subcarriers	4
OFDM Symbol duration	4 μs
Guard Interval	800 ns

B. Model verification

To test the validity of the proposed channel model, packet-error-rate (PER) simulations were carried using the set of measured channel realizations. An example of the results is given in Fig. 3, which shows PER curves for a 3×3 configuration, applying QPSK modulation and rate 1/2 JC, resulting in 36 Mbps. The packet length was 64 byte. The 3×3 channel matrices were found from the measured 4×4 channel matrices, by removing elements corresponding to the fourth TX branch and elements corresponding to the fourth RX branch. Simulations were also carried out with the channel model of Section II for rms delay spreads of 10 ns, 30 ns, 50 ns and 100 ns.

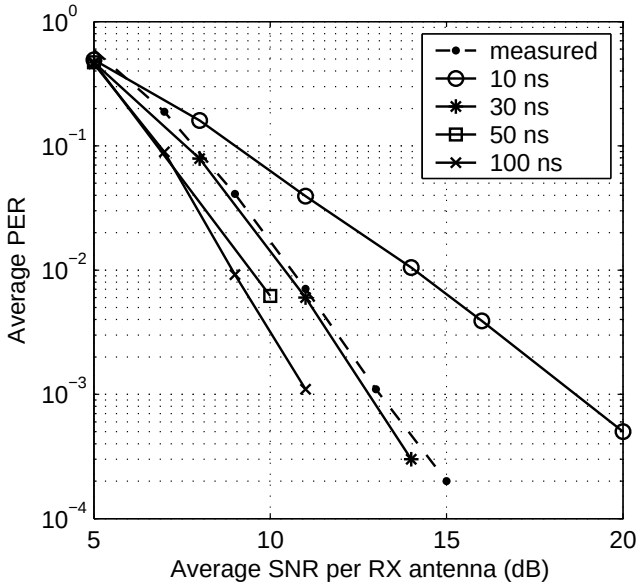

Fig. 3. Results from PER simulations for a 3×3 configuration for QPSK, rate 1/2 conv. coding (36 Mbps), MMSE detector, 64 byte packets, measured and simulated channels.

Figure 3 shows the performance of link-level simulations with the measured channel set is close to the performance with simulated channels with an rms delay spread of 30 ns. Results for other detection algorithms and antenna configurations are similar. It is noted, however, that although the curves reveal a diversity order similar to the 30 ns curve in most cases, some curves show a right-shift of several dBs compared the 30 ns curve. This might be explained by the fact that the channel correlation was not taken into account or by the fact that the tail of the measured PDPs distribution is not exactly exponentially decaying. Thus the assumption of a exponential decaying PDP made in modelling the channel is not fully valid. Nevertheless, all PER curves from measured channels lie between the curves corresponding to the simulated channels with 10 and 50 ns rms delay spread. This confirms that the channel model is useful for evaluation of the MIMO OFDM system and that the approach taken in this paper is valid.

C. Simulation results

Now that the channel model has been validated, MIMO configurations and detection algorithms can be evaluated using it. Here only the most important of the numerous results are shown.

Figure 4 shows the PER performance as function of the average signal to noise ratio (SNR) for a system experiencing a wireless channel with an rms delay spread of 50 ns. The simulated system has 3 TX and 3 RX branches, denoted as 3×3, and applies QPSK modulation. The rate of the convolutional encoder is 1/2, resulting in a data rate of 36 Mbps. Results are shown for VBLAST, MLD, MMSE and ZF based detection. The VBLAST scheme applies PAC, while the others apply JC. Note that the PAC VBLAST is implemented as proposed in [16], where the detection of the $(n+1)$th layer uses the re-encoded and remodulated output of the Viterbi decoder of the nth layer.

Furthermore, the figure includes results for two single-input single-output (SISO) systems. The first one, denoted by "1×1, 1/3", applies QPSK modulation and convolutional coding of rate 1/2. It thus reaches the same rate per branch as the 3×3 system, but 1/3 of the total data rate, i.e., 12 Mbps. The second configuration, denoted by "1×1", applies 16QAM modulation and convolutional coding of rate 3/4. Here the rate per branch is higher, but the total data rate is equal to that of the MIMO system, i.e., 36 Mbps.

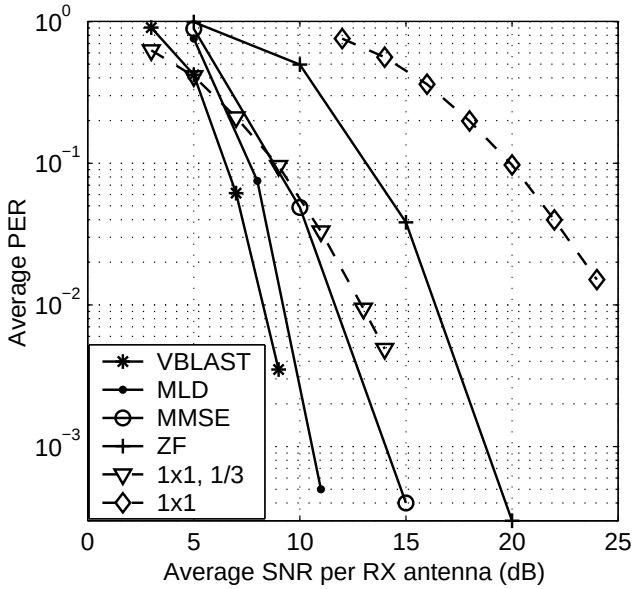

Fig. 4. Results from PER simulations for a 3×3 configuration for QPSK, rate 1/2 conv. coding (36 Mbps), 1000 byte packets, rms delay spread = 50 ns, different detectors. Corresponding curves for SISO systems with equal branch rate (*1×1, 1/3*) and equal data rate (*1×1*)

It can be concluded from Fig. 4 that for the regarded SNR range VBLAST performs best. This can be explained by the frequency diversity, which can be better exploited by the PAC scheme than by the JC scheme. The ZF detector requires a SNR which is about 5 dB higher than that required by the MMSE detector to reach the same PER performance.

When comparing the MIMO performance to that of the SISO cases, it is clear that VBLAST and MLD perform even better then the 1×1 system with 1/3 of the data rate. For low PER values, also the MMSE detector performs better, but the ZF detector is always worse than this SISO case. The SISO scheme with the same data rate, i.e., 16QAM and coding rate 3/4, needs a 7.8, 11.8, 14.2 and 15.1 dB higher SNR to reach a PER of $2 \cdot 10^{-2}$ than the ZF, MMSE, MLD and VBLAST based detector, respectively.

Figure 5 compares results for a 2×2 and a 2×3 configuration experiencing a channel with a rms delay spread of 30 ns. The modulation is 64QAM and the coding rate of the convolutional code is 3/4, which corresponds to a data rate of 108 Mbps. Again the VBLAST scheme applies PAC, while the others apply JC.

Again the performance of PAC VBLAST is not far from the MLD performance, but it is not superior as observed in Fig. 4. This is due to the lower frequency diversity, since the delay spread is smaller. The ZF and MMSE detector show the same performance for these high SNR values. Nevertheless, the complexity analysis of the detection algorithms in [14] shows that the complexity of MLD for 64QAM prohibits a cost-effective implementation. ZF and MMSE are, however, very well implementable. The complexity of PAC VBLAST is only linearly greater than that of ZF and MMSE. The disadvantage of PAC VBLAST, however, is its latency, since the data has to pass through a decoder and encoder for every TX branch.

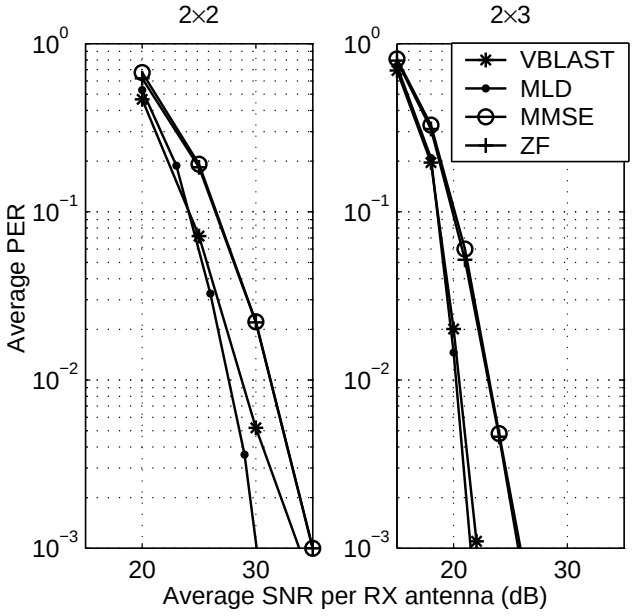

Fig. 5. Results from PER simulations for a 2×2 and 2×3 configuration for 64QAM, rate 3/4 conv. coding (108 Mbps), 64 byte packets, rms delay spread = 30 ns.

Additionally, we can conclude from Fig. 5 that adding an extra RX antenna, e.g., 2×3, drastically improves the performance of all MIMO schemes. At a PER of 10^{-2} the extra antenna gains 9.2, 9.2, 7.4 and 8.2 dB for the ZF, MMSE, MLD and VBLAST based detector, respectively. Also note that the ZF bases 2×3 scheme performs 5 dB better in SNR than the MLD bases 2×2 scheme at this target PER. From this it might be concluded that adding an extra RX branch might be beneficial for keeping the performance at a good level and the required computational complexity manageable, since a low complex detection scheme can be chosen.

From the link-level simulation results we on the whole conclude that PAC VBLAST is the preferable detection method, since it gives high performance, but low complexity. When the corresponding latency, however, is not tolerable, the MMSE based detection is proposed, where it is noted that adding an additional RX branch drastically improves performance.

V. System level throughput

Results from the link-level simulations reported in the the previous section, were used to create PER tables. In this section, an estimation of the throughput in a system with an access point (AP) and multiple MIMO user terminals (UTs) is made. For this purpose, a network system model is developed based on an analytical approach proposed in [11]. The PER tables are linked to the network model.

Since all users in a 802.11 based cell apply carrier sense multiple access/collision avoidance (CSMA/CA) to access the wireless medium and hidden node situations are not regarded, the assumption is made that there is no interference in the single radio cell layout, making the performance purely limited by the signal strength and the background noise.

The assumption is made that perfect transmit power control (TPC) is applied. However, the power of the UT is usually limited to a certain maximum value. This means that the RX power will start to drop above a certain distance between AP and UT, which will result in a decreased SNR. It can happen that a lower data rate has to be chosen to keep the PER at an acceptable level, i.e., applying link adaptation (LA). This clearly shows LA and TPC are not independent.

A. Link Adaptation

To explain the LA concept we regard the throughput experienced by the user $\mathcal{T}$, which is a function of the maximum achievable data rate R and the PER, and is defined as

$$\mathcal{T} = R \cdot \{1 - \text{PER}(\gamma)\} \quad , \tag{1}$$

where γ denotes the SNR per branch. Please note that all system parameters are included in the throughput since R and PER depend on the fast-fading channel model with the link adaptation scheme and γ depends on the power control and the slow-fading path loss model.

In Fig. 6 the maximum achievable throughput, as function of the average SNR per RX antenna is depicted for a 2×2 MIMO OFDM system. For simplicity we consider a system with only 4 rates: 64QAM - rate 3/4 (108 Mbps), 16QAM - rate 3/4 (72 Mbps), QPSK - rate 3/4 (36 Mbps) and QPSK - rate 1/2 (24 Mbps). All apply the MMSE based detector.

To be able to cope with variations in the quality of the radio link, the AP is able to select different PHY modes for both

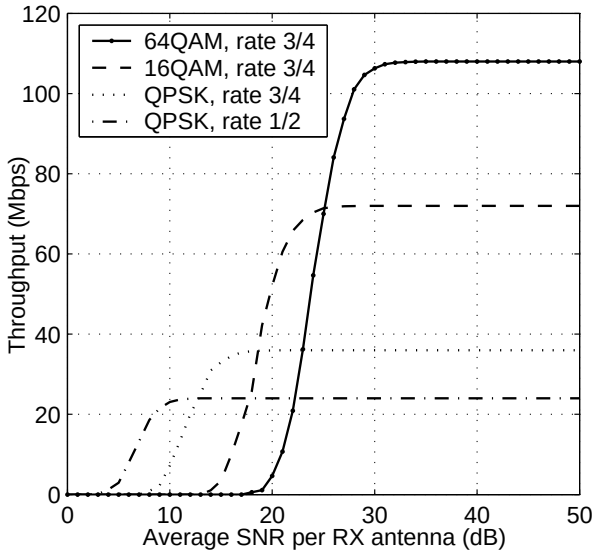

Fig. 6. Maximum throughput versus average SNR of the chosen modes for a MMSE 2×2 system.

down- and uplink. A LA scheme now selects the envelope of the curves in Fig. 6 to maximize the throughput as function of the SNR.

B. Transmit Power Control

To model the path loss in the cell we apply a two slope model, which is based on the assumption, that for distances up to 5 m from the TX, a line of sight path would exist, whereas for high distances obstacles can be excepted, increasing the path loss coefficient [11]. The path loss for distances up to 5 m is 20 dB per decade and for distances higher than 5 m, this is 35 dB per decade. In the two regions a fixed loss of 46 and 36 dB is assumed, respectively. A minimum separation between UT and AP of 2 m is assumed. Furthermore, it is assumed that the background noise N_0 has a level of -95 dBm.

The transmit power control is assumed to work in such a way that the AP announces its downlink (DL) transmit power $P_{t,AP}$ and the expected uplink (UL) reception power $P_{e,AP}$ in every medium access control (MAC) frame. The UT can calculate the path loss L from the reception power $P_{r,UT}$ and the known AP transmit power $P_{t,AP}$. The required transmit power is then given by

$$P_{t,UT} = P_{e,AP} + L \ , \tag{2}$$

where $P_{t,UT}$ is limited by $P_{t,UT,\max}$. In this work we will set $P_{t,UT,\max}$ equal to 23 dBm.

Using the path loss model we find an expression for the transmit power of the UT

$$P_{t,UT} = \begin{cases} P_{e,AP} + 46 + 20\log_{10}(d) & 2 \le d < 5m \\ P_{e,AP} + 36 + 35\log_{10}(d) & 5 \le d \le d_{\max} \\ P_{t,UT,\max} & d_{\max} < d \end{cases} , \tag{3}$$

where d is the distance between AP and UT in meters and $d_{\max} = 10^{(P_{t,UT,\max}-36-P_{e,AP})/35}$. From this expression also the received power at the AP $P_{r,AP}$ can be calculated. Clearly, this will be equal to $P_{e,AP}$ for distances smaller than $d_{\max}$ and it will follow the decreasing tendency of the path loss for higher distances.

C. Cell throughput

The next step is to derive the pdf $\mathrm{f}_{\gamma_{AP}}(\gamma_{AP})$ of the SNR at the AP γ_{AP}. UTs are assumed to be uniformly distributed in a circle with radius ρ around the AP. The pdf of the SNR is derived from the pdf of the distance d of the UTs from the AP and the earlier described path loss model is then given by [11]

$$\mathrm{f}_{\gamma_{AP}}(\gamma_{AP}) = \mathrm{f}^{(1)}_{\gamma_{AP}}(\gamma_{AP}) + \mathrm{f}^{(2)}_{\gamma_{AP}}(\gamma_{AP}) \ , \tag{4}$$

where

$$\mathrm{f}^{(1)}_{\gamma_{AP}}(\gamma_{AP}) = \min\left\{1, \frac{1}{\rho^2-4}\left(10^{Y}-4\right)\right\} \cdot \delta(\gamma_{AP} - (P_{e,AP} - N_0)) \ , \tag{5}$$

where $Y = 2(P_{t,UT,\max} - 36 - P_{e,AP})/35$, $\delta(\cdot)$ denotes the Dirac impulse function and

$$\mathrm{f}^{(2)}_{\gamma_{AP}}(\gamma_{AP}) = \frac{2\ln 10}{35(\rho^2-4)}\left(10^{X}-4\right) \ , \tag{6}$$

for $P_{r,AP}(\rho) - N_0 \le \gamma_{\mathrm{AP}} < P_{e,AP} - N_0$ and otherwise $\mathrm{f}^{(2)}_{\gamma_{AP}}(\gamma_{AP}) = 0$. Here $X = 2(P_{t,UT,\max} - 36 - \gamma_{AP} - N_0)/35$.

With the pdf of the SNR, we can now calculate the achievable throughput. For this purpose, we have to determine the time during which the radio resource is used with a certain rate. This time share is determined by the scheduling algorithm in the MAC layer of the system, which meets the decision on who uses the radio resource when and for how long. Let R_{PM} be the maximum possible data rate of the PHY mode PM and $\max_\gamma(PM)$ the PHY mode with the highest throughput for a given SNR, i.e., the PHY mode chosen by the LA algorithm. R_{PHY} is the data rate of the PHY mode with the highest data rate. The time normalization factor τ_n is then defined as [11]

$$\tau_n = \int_0^\infty f_{\gamma_{AP}}(\gamma_{AP}) \sqrt{\frac{R_{\mathrm{PHY}}}{R_{\max_{\gamma_{AP}(PM)}}}} d\gamma_{AP} \ . \tag{7}$$

If $\mathcal{T}_{PM}(\gamma_{AP})$ represents the throughput for a given γ_{AP} and the selection of the PHY mode PM according to the theoretical throughput curves, the expected value of the maximal throughput $\mathcal{T}_{\max}$ is given by

$$E(\mathcal{T}_{\max}) = \frac{1}{\tau_n}\int_0^\infty f_{\gamma_{AP}}(\gamma_{AP})\mathcal{T}_{\max(PM)}(\gamma_{AP}) \cdot \sqrt{\frac{R_{\mathrm{PHY}}}{R_{\max_{\gamma_{AP}(PM)}}}} d\gamma_{AP} \ . \tag{8}$$

Now using the LA curves as derived in Section V-A, which are based on the link-level simulation PER results, and the pdf of the SNR as given by (4), we can calculate the mean achievable throughput for different configurations.

Figure 7 shows the achievable throughput for a 2×2 MMSE based MIMO system as function of the cell radius. The rates vary from 24 Mbps to 108 Mbps. It is clear that the achievable throughput depends on the expected receive power at the AP $P_{e,AP}$. When the expected RX power is too low, the highest rate will never be reached and the throughput is limited to a lower level.

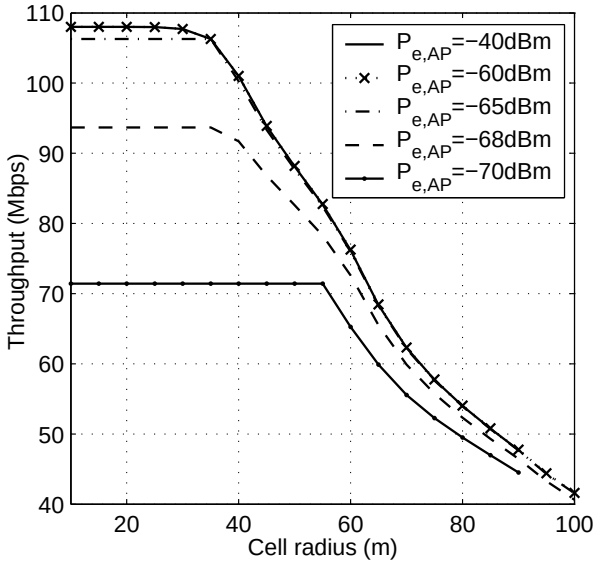

Fig. 7. Maximum throughput 2x2 MMSE MIMO versus cell radius in the uplink. Expected RX power at the AP $P_{e,AP}$ is varied.

Figure 8 compares the achievable throughput of the 2×2 MMSE MIMO system to the corresponding results for a SISO 802.11a system. The SISO systems has rates varying from 6 Mbps to 54 Mbps. Although the negative slope of the throughput versus distance is higher for the MIMO system than for the SISO system, the throughput gain of using MIMO is substantial, ranging from a factor of 1.5 to 2 for the regarded range of cell radii.

It is noted that this analysis does not take into account the overhead of the control traffic, MAC control and convergence layer. To obtain the real maximum throughput, the achievable throughput as found above has to be multiplied with a factor depending on the overhead. For 802.11a networks this will typically be 0.7 or lower.

VI. Conclusions

The paper discusses the throughput of a multiple-input multiple-output orthogonal frequency division multiplexing (MIMO OFDM) based wireless local-area-network (WLAN) system. From broadband MIMO channel measurements a channel model is derived. This channel model is used for link-level simulations with different MIMO configurations. It is concluded that PAC VBLAST is well applicable, when the latency is acceptable. Applying systems with an extra receiver antenna and low computational complexity algorithms, like MMSE, is shown to have better performance than the highly complex MLD without this extra branch.

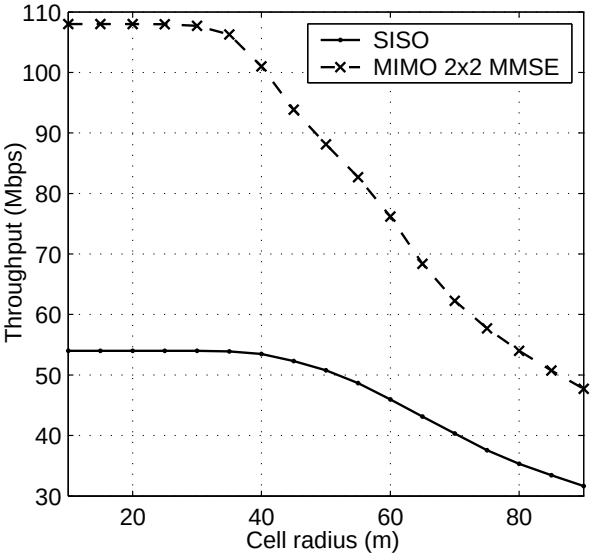

Fig. 8. Throughput comparison between SISO and 2x2 MMSE MIMO versus cell radius in the uplink. Expected RX power at the AP $P_{e,AP}$ is -40 dBm.

The PER tables are used to calculate the throughput of a single cell system applying link adaptation and transmit power control. From the results for an example with a 2×2 MMSE system, it is concluded that the gain of MIMO is substantially, but decreases with increasing cell radius.

Acknowledgements

This work was carried out within the B4 Broadband Radio@hand project, which is supported in part by the Dutch Ministry of Economic Affairs under grant BTS01063. The authors thank Allert van Zelst and Manel Callodos for their input to this paper.

References

[1] G.J. Foschini and M.J. Gans, "On limits of wireless communications in a fading environment when using multiple antennas," *Wireless Personal Communications*, vol. 6, no. 3, pp. 311–335, March 1998.

[2] I. Telatar, "Capacity of multi-antenna gaussian channels," *European Trans. on Telecommun.*, vol. 10, pp. 585–595, Nov./Dec. 1999.

[3] G.G. Raleigh and V.K. Jones, "Multivariate modulation and coding for wireless communication," *IEEE Journ. on Selected Areas in Commun.*, vol. 17, no. 5, pp. 851–866, May 1999.

[4] *IEEE 802.11a standard*, ISO/IEC 8802-11:1999/Amd 1:2000(E).

[5] *IEEE 802.11g standard*, Further Higher-Speed Physical Layer Extension in the 2.4 GHz Band.

[6] H. Sampath, S. Talwar, J. Tellado, V. Erceg, and A. Paulraj, "A fourth-generation mimo-ofdm broadband wireless system: design, performance, and field trial results," *IEEE Commun. Magazine*, vol. 40, no. 9, pp. 143–149, Sep. 2002.

[7] P.W. Wolniansky et al., "Prototype experience for mimo blast over third-generation wireless system," *IEEE Journ. on Selected Areas in Commun.*, vol. 21, no. 3, pp. 440–451, April 2003.

[8] A. van Zelst and T.C.W. Schenk, "Implementation of a mimo ofdm-based wireless lan system," *IEEE Trans. on Sign. Proc.*, vol. 52, no. 2, pp. 483–494, Feb. 2004.

[9] B. Vandewiele and P. Mattheijssen, "An experimental broadband 4x4 mimo test-bed," in *Proc. of URSI XXVIIth General Assembly*, Aug. 2002, pp. 1–4.

[10] B.E. Braswell and J.C. McEachen, "Modeling data rate agility in the ieee 802.11a wlan protocol," in *Proc. OPNETWORK2001*, 2001.

[11] M. Radimirsch and K. Jobmann, "System model for wireless data networks," in *Proc. COST 273 TD(03)004, Barcelona, Spain*, Jan. 2003.

[12] M. Zorzi, "On the capture performance of smart antennas in a multicellular environment," *IEEE Trans. on Commun.*, vol. 50, pp. 536–539, April 2002.
[13] G. Dolmans and M. Collados, "Broadband measurement analysis of indoor space-time channels," in *Proc. of URSI XXVIIth General Assembly*, Aug. 2002, pp. 1–4.
[14] A. van Zelst, *MIMO OFDM for Wireless LANs*, Ph.D. thesis, Eindhoven University of Technology, April 2004.
[15] E. Martijn et al., "Broadband radio@hand deliverable 2.2: Development of propagation models for umts and wlan, preliminary results," Tech. Rep., June 2003, available at: http://tte.ele.tue.nl/radio/.
[16] A. van Zelst, "Per-antenna-coded schemes for mimo ofdm," in *Proc. IEEE International Conference on Communications 2003*, May 2003, vol. 4, pp. 2832–2836.